International Journal of Pharmacology

ISSN 1811-7775

science alert

ansinet
Asian Network for Scientific Information

OPEN ACCESS International Journal of Pharmacology

ISSN 1811-7775
DOI: 10.3923/ijp.2020.542.553

Research Article
Chlorogenic Acid Inhibits LPS-Induced Mammary Epithelial Cell Inflammation in Mice by Targeting CD14 and MD-2

[1,2]JunChao Peng, [3]YuKun Wang, [4]XueYan Xie, [2]Qiong Yi, [5]Xin Li, [3]YuHao Wei, [1]XuHua He and [1,2]Lu Wang

[1]College of Pharmacy, Guizhou University, Guiyang Guizhou, People's Republic of China
[2]Southwest Biomedical Resources of the Ministry of Education, Guizhou University, Guiyang Guizhou, People's Republic of China
[3]Shandong New Time Pharmaceutical Company, Lunan Pharmaceutical Group, Linyi Shandong, People's Republic of China
[4]First Clinical Medical College, Zunyi Medical University, Zunyi Guizhou, People's Republic of China
[5]Xishui County Animal Husbandry Bureau, Zunyi Guizhou, People's Republic of China

Abstract

Background and Objective: Both leukocyte differentiation antigen 14 (CD14) and myeloid differentiation protein-2 (MD-2) contain hydrophobic vesicles for extracting and delivering lipopolysaccharide (LPS), which play an irreplaceable role in the extracellular signal transduction of LPS. Chlorogenic acid (CGA) is a phenolic compound with a strong anti-inflammatory effect. However, it is currently unclear whether CGA blocks the extracellular signal transmission of LPS by occupying the hydrophobic pockets of CD14 and MD-2. **Materials and Methods:** Flow cytometry and siRNA were used to detect the presence of CD14 and MD-2 on breast epithelial cells (MECs). Molecular docking, Western blot, reverse transcription-polymerase chain reaction and enzyme-linked immunosorbent assay were used to study the targeting effect of CGA on CD14 and MD-2 and its influence on cytokine secretion. The protective effect of CGA on breast inflammation was observed under a transmission electron microscope. **Results:** The results showed that MD-2 and CD14 were expressed on MECs. When CD14 and MD-2 are inhibited alone or at the same time, the binding rate of LPS and MECs and the secretion of cytokines are reduced. CGA can not only occupy the hydrophobic vesicles of CD14 and MD-2, block the extracellular signal transmission of LPS but also inhibit the expression of CD14 and MD-2, thereby blocking the signal transmission of LPS from extracellular to intracellular. **Conclusion:** Besides, CGA can effectively inhibit the general changes of breast tissue, breast inflammatory cell infiltration, mitochondria and rough endoplasmic reticulum damage caused by lipopolysaccharide. In conclusion, CGA is expected to act as an antagonist of CD14 and MD-2 to inhibit mastitis.

Key words: CD14, MD-2, chlorogenic acid, TLR4 signaling pathway, lipopolysaccharide, mammary epithelial cells, mastitis

Citation: Peng, J.C., Y. Wang, X.Y. Xie, Q. Yi, X. Li, Y.H. Wei, X.H. He and L. Wang, 2020. Chlorogenic acid inhibits LPS-induced mammary epithelial cell inflammation in mice by targeting CD14 and MD-2. Int. J. Pharmacol., 16: 542-553.

Corresponding Author: Lu Wang, College of Pharmacy, Southwest Biomedical Resources of the Ministry of Education, Guizhou University, Guiyang Guizhou, China

Competing Interest: The authors have declared that no competing interest exists.

Data Availability: All relevant data are within the paper and its supporting information files.

INTRODUCTION

CD14 is a GPI-anchored glycoprotein with 22 leucine-rich repeats and a typical horseshoe-shaped structure[1]. The NH_2-terminal side of the CD14 has a hydrophobic pocket with a cluster of positively charged residues at the edge, which can probably accommodate acylated ligands, such as phosphorylated lipid part A[2,3]. MD-2 is a soluble protein that has been reported to act both as a chaperone for surface expression of TLR4 and as a critical protein in agonist-dependent TLR4 signaling, MD-2 binds to the extracellular domain of TLR4 to form stable TLR4 receptor complexes and is essential for TLR4-mediated responses to LPS[4-6]. Similar to CD14, MD-2 shows a deep hydrophobic cavity sandwiched by two β sheets to hold most of the lipid portion of LPS. Both CD14 and MD-2 extract and recognize LPS through the hydrophobic pocket and then transmit LPS to TLR4, which innately recognizes the receptor, then activates the intracellular signal, causes the release of cytokines and then cause inflammation[7,8].

LPS is an outer membrane glycol-lipid of Gram-negative bacteria and a well- known inducer of the innate immune response[1]. It is composed of a hydrophobic lipid A component and the hydrophilic polysaccharides of the core and O-antigen[9]. The lipid A portion represents part of the conserved molecular pattern of LPS and is responsible for most of the LPS-induced biological responses[10]. In the crystal structure, lipid A contains six aliphatic chains, five of which are buried deep in the hydrophobic pocket of MD-2 and the other is exposed on the surface of MD-2 which makes up the core hydrophobic interface and interacts with the extracellular domain of adjacent TLR4 molecules[11]. Additionally, the phosphate groups of lipid A interact with positively charged amino acids of TLR4. By simultaneously binding to MD-2 and to the adjacent TLR4 receptor, LPS facilitates the formation of "M" shaped dimers of TLR4/MD-2 complexes, which will activate the TLR4 signaling pathway[12,13].

CGA is a phenolic compound found in medicinal plants, including Angelicae Sinensis Radix, Chuanxiong Rhizoma, Eucommia ulmoides and honeysuckle and also presented in wine, tea and coffee[14]. It is reported to have anti-inflammatory, anti-virus, anti-oxidation, hypolipidemic and blood glucose effects as well as enhancing immunity and other biological systems[15]. Previous studies reported that CGA regulated the release of cytokine and chemokine to protect against acute lung injury induced by LPS and protected the LPS-challenged animals by suppression of hepatic TLR4 mRNA expression[16,17]. In addition to its antioxidant effects, CGA suppressed cellular apoptosis and blocked the activation of nuclear factor NF-κB, activator protein AP-1 and mitogen-activated protein kinase (MAPK) *in vitro*[18]. CGA has a broad anti-inflammatory effect and has many intracellular molecular targets. However, it has not been reported whether CGA acts on extracellular targets CD14 and MD-2 and it is unclear whether CGA inhibits the production of inflammation by targeting CD14 and MD-2 to block LPS extracellular signaling[19,20]. Therefore, this study used CD14 and MD-2 as molecular targets to study the anti-inflammatory effects of CGA.

MATERIALS AND METHODS

Study area: The study was carried out at Biochemical Engineering Center, Guizhou University, China from February, 2017-September, 2019.

Cell cultures: The procedure for the primary culture of MECs was previously described[21]. The mouse MECs were cultured in DME/F-12 medium (HyClone) supplemented with 10% heat-inactivated fetal calf serum (IBL), 1 μg mL^{-1} rhEGF (Sigma), 2.5 μg mL^{-1} Insulin (Sigma), 1 μg mL^{-1} cholera toxin (Sigma), 1 μg mL^{-1} Hydrocortisone, 29.2 μg mL^{-1} L-Glutamine (Sigma) and 1 IU mL^{-1} penicillin and streptomycin (Gibco). The cells were maintained at 37°C in a humidified atmosphere containing 5% CO_2 in an incubator (Thermo Scientific, USA).

Flow cytometry: The MECs were inoculated into 24-well cell culture plates. After the cells were grown to uniform monolayer cells, they were randomly divided into the control group, CD14 incubated group and MD-2 incubated group. The primary antibodies of anti-CD14 (Sigma, dilution 1:100) and anti-MD-2 (Sigma, dilution 1:100) were diluted in labeled Eppendorf tubes were and were added to each well for 30 min at 4°C. After the incubation was completed, it was gently washed three times with PBS. Incubate with 10% sheep serum blocking solution for 10 min at room temperature, then wash the sheep serum with PBS and the CD14 incubated group added secondary antibody anti-rat lgG-Alexa 594 (Sigma, diluted 1:200) and the MD-2 incubated group added anti-Rabbit lgG-Alexa 488 (Sigma, diluted 1:200), incubate for 1 h at room temperature in the dark and washed with PBS three. The control group except for the primary antibody and secondary antibody were not added, the other operations were the same. Then cells were cooled at 4°C for 10 min, centrifuged at 1000 rpm for 2 min and washed with PBS twice. The final cell suspension was used to measure the fluorescence intensity by flow cytometry assay. (Beckman, USA).

RNAi: RNAi was carried out as previously described[22]. Briefly, mouse MECs were prepared and inoculated with an appropriate number of mouse MECs into 24-well cell culture plates. Pools of three small interfering RNA (siRNA), duplexes/gene (Invitrogen) were transfected into MECs, they were randomly divided into control group, LPS group, MD-2 siRNA group, CD14 siRNA group and CD14+MD-2 siRNA group with 3 replicates in each group, 24 hrs after siRNA transfection, fluorescent LPS (Sigma) was added to a final concentration of 5 μg mL^{-1} each group for 12 hrs except the naked siRNA group. The final cell suspension was used to measure the fluorescence intensity by flow cytometry assay and used fluorescence intensity (gate%×X mean) to show the FITC-LPS binding ability.

ELISA: To assess the importance of CD14 and MD-2 for the secretion of IL-1β, TNF-α and IL-6 and the effect of CGA (Changsha Staherb Natural Ingredients Co., Ltd., Changsha, China) on TNF-α and IL-6 secreted by MECs, cell suspensions (5×10^4 cell/well) were added into 96-well plates, the MECs were treated according to the above siRNA method or according to the results of the cytotoxicity test, the final concentrations of CGA were 20, 200 and 2000 μg mL^{-1} co-culture for 12 hrs with LPS (10 μg mL^{-1}) (Sigma), respectively. Culture supernatants were collected by centrifugation and levels of IL-1β, TNF-α and IL-6 were measured using cytokine-specific ELISA kits (ColorfulGene Biological Technology Co. Ltd, Wuhan, China) according to the manufacturer's instructions.

Molecular docking study: The study was performed under CDOCKER and LibDock protocol of Discovery Studio 2017 R2. The 3D structure of CGA was generated and minimized, the crystal structures of CD14 (PDB1WWL) and MD-2 (PDB2Z64) were obtained from Protein Data Bank, they were optimized by hydrogenation, dehydration and CHARMm force field, the CGA was placed into the LPS binding region at the NH_2-terminal of CD14. Similarly, MD-2 protein was defined as the receptor and the site sphere was selected on the hydrophobic cavity of MD-2 and then CGA was placed. Molecular docking scoring is obtained by CDOCKER and LibDock program, respectively. The types of interactions between proteins and CGA were analyzed at the end of the molecular docking[23,24].

MTT assay: To determine the appropriate CGA stimulation amount, an MTT assay was used to measure cell proliferation[25]. The cell concentration of MECs was adjusted to 5×10^4 cell/well and then cells were transferred into 96-well plates and cultured for 12 hrs. CGA was prepared as 11 concentrations and added to wells (0.015625–512 mg mL^{-1}). Four wells without CGA were used as a normal control in each plate. MECs were treated with different concentrations of CGA for 24 hrs. Subsequently, 20 μL of MTT solution (5 mg mL^{-1}) was added to each well and incubated for 4 hrs. After washing the supernatant out, an insoluble formazan product was dissolved in DMSO. The optical density of the 96-well culture plates was then measured at 490 nm absorption wavelength. The optical density of formazan formed in untreated control cells was used to indicate 100% viability. The concentrations of CGA that resulted in 50% cell death (IC_{50}) in the monolayer cultures were determined from dose-response curves. The assay was carried out with 4 replicates for each culture.

qRT-PCR: To determine the effect of CGA on the mRNA expressions of CD14 and MD-2 in MECs, 1000 μL MEC suspension was added into a 12-well plate. When cells had filled the well, 1000 μL CGA (20, 200 and 2000 μg mL^{-1}) and/or LPS(10 μg mL^{-1}) solution were added to the MECs. After 24 hrs incubation, each group of MECs was harvested and the RNAs were isolated by following the manufacturer's instructions. All RNAs were reverse transcribed by a real-time Polymerase Chain Reaction (PCR) kit. The resulting cDNA was stored at -80°C until amplification.

All primers (Table 1) used in this study were designed using the 'Primer Premier 5.0' software using publicly available mouse sequences and were purchased from NCBI. Relative quantities of gene transcripts were measured by qPCR using the Power SYBR™ Green PCR Master Mix (Thermo Scientific). Two microliters of each cDNA template were amplified in a 10 μL reaction volume at the following conditions: preheating at 95°C for 3 min earliest annealing for 30 sec, 58.3°C (CD14)

Table 1: Gene-specific oligonucleotide primers used for qPCR

	Oligonucleotides (5'-3')				
Gene symbol	F: forward	R: reverse	Amplicon (bp)	Annealing temperature (°C)	Accession number (GenBank)
CD14	F:AGCACACTCGCTCAACTTTTC	R:GCCCAATTCAGGATTGTCAGAC	88	58.3	NM_009841
MD-2	F:GAATCTGAGAAGCAACAGTGGT	R:CTCAACATGCACAAATCCATTGG	144	58.8	NM_016923
GAPDH	F: GCAACTCCCACTCTTCCA	R: GCTCAGGGTTTCTTACTCC	158	--	NM_008084

or 58.8°C (MD-2) for 30 sec, 72°C for 30 sec, for 40 cycles, with a final extension at 72°C for 2 min. For the quantitative evaluation of gene expressions, CD14 and MD-2 mRNA levels were normalized to GAPDH mRNA by the 2^{-Ct} method[26].

Western blot: After cells were cultured for the indicated times, they were collected and washed twice with cold D-Hanks. Total protein was extracted by using RIPA buffer. The protein concentrations were determined by using the BCA method. The proteins (20 μg) were separated through 10% SDS-PAGE and subsequently transferred to PVDF membranes. The membranes were blocked with 5% skim milk containing 0.01% (v/v) Tween-20 in TBST for 1 h at room temperature and were then incubated with a monoclonal rabbit CD14 antibody (Cell Signaling Technology, dilution 1:1000) or with a monoclonal rabbit MD-2 antibody (Novus Biologicals, dilution 1:300) overnight at 4°C. The membranes were washed three and incubated with the secondary antibodies (Epizyme, dilution 1:50000) for 1 h at room temperature. The protein bands were detected with a chemiluminescence western blot detection system.

Animals: Kunming mice (No. SCXK (Yu) 2012-0011) were purchased from the experimental animal center of the Third Military Medical University of PLA. All mice were clinically healthy and kept under standard environmental conditions of temperature (24±2). The animals had free access to water and a standard diet. This study was performed under the Research Ethics Committee of Guizhou Medical University (Approval Number: No.1800756).

Histopathologic evaluation of mammary gland tissue: The mammary inflammatory model was performed as described by Zhang[27]. Briefly, 10-12-week old mid-pregnant Kunming mice were used. To establish the mouse model of mammary inflammation, 25 μL of 0.2 mg mL^{-1} LPS was inoculated via the udder canal through the L4 (left) and R4 (right) abdominal mammary glands. Control mice received PBS. First, the mice were intraperitoneally administered with CGA injection and then LPS was injected 12 hrs later. The control group and LPS group were intraperitoneally injected with an equal volume of PBS. At 24 hrs after LPS injection, the animals were sacrificed. The mammary gland tissue was harvested and fixed in 4% paraformaldehyde for 24 hrs, embedded in paraffin, cut into 5 μm thick serial sections and then stained with Hematoxylin and Eosin (HE) for light microscopy. Other mammary gland tissues were used for TEM to study the ultrastructural changes of cells. The tissues were fixed with 2.5% glutaraldehyde in 0.1 mol L^{-1} phosphate buffer for 2 hrs and postfixed in 1% osmium tetroxide in 0.1 mol L^{-1} phosphate buffer for 1 h. Then, the samples were dehydrated using a series of ethanol solutions in the order of concentration of 30, 50, 70, 80, 90, 95 and 100%. After dehydrating and embedding in Spurr's Resin, thin sections were cut and double-stained with uranyl acetate and lead citrate. The grids were examined with JEM-1230 TEM (JEOL, Japan).

Statistical analysis: SPSS 17.0 software (Chicago, IL, USA) was used for statistical analysis. The data were expressed as the mean±standard deviation (SD) and analyzed by one-way ANOVA. A comparison between the groups was made by analyzing data with posthoc method. Differences were considered significant at $p<0.05$.

RESULTS

Protein expression of CD14 and MD-2 in MECs by flow cytometry: The levels of CD14 and MD-2 expression of cell surface were examined by Flow analysis (Fig. 1a, b). Fluorescence intensity after incubation with anti-CD14 and anti-MD-2 antibody was significantly stronger than the blank group. Based on the flow results, the presence of CD14 and MD-2 in MECs cells will be the basis for the following studies.

Effect of CD14 and MD-2 gene silencing on mouse MECs binding rate: Effect of CD14 and MD-2 siRNA on the specific binding of LPS with MECs. The peak of the LPS group shifted to the right a little and the fluorescence intensity data was increased with statistical significance ($p<0.01$) (Fig. 2). After CD14 and MD-2 siRNA treatment, the increased fluorescence intensity of flow cytometry result was reduced ($p<0.01$), which may be the antagonistic effect of CD14 and MD-2 on the binding of LPS to the cell membrane receptor. These findings suggested that the importance of CD14 and MD-2 for LPS on the cell membrane.

Effect of CD14 and MD-2 gene silencing on the cytokine of IL-1β, TNF-α and IL-6: To confirm that CD14 and MD-2 play important roles in the signaling pathway of the extracellular LPS to TLR4 segment of MECs, we detected the levels of IL-1β TNF-α and IL-6. Results showed that LPS could stimulate the secretion of IL-1β, TNF-α and IL-6 on MECs ($p<0.01$) and silencing CD14 and MD-2 genes can significantly inhibit the release of IL-1β, TNF-α and IL-6, respectively ($p<0.05$, $p<0.01$) (Fig. 3).

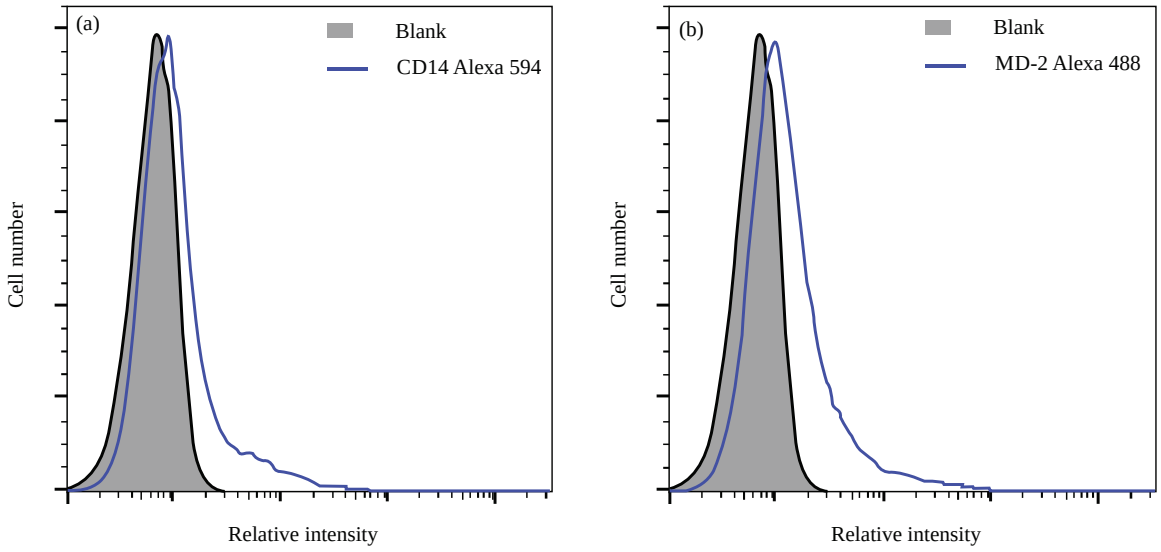

Fig.1(a-b): Relation fluorescence intensity of CD14, MD-2 protein expression on MECs by flow
A: Incubated with CD14 and B: Incubated with MD-2

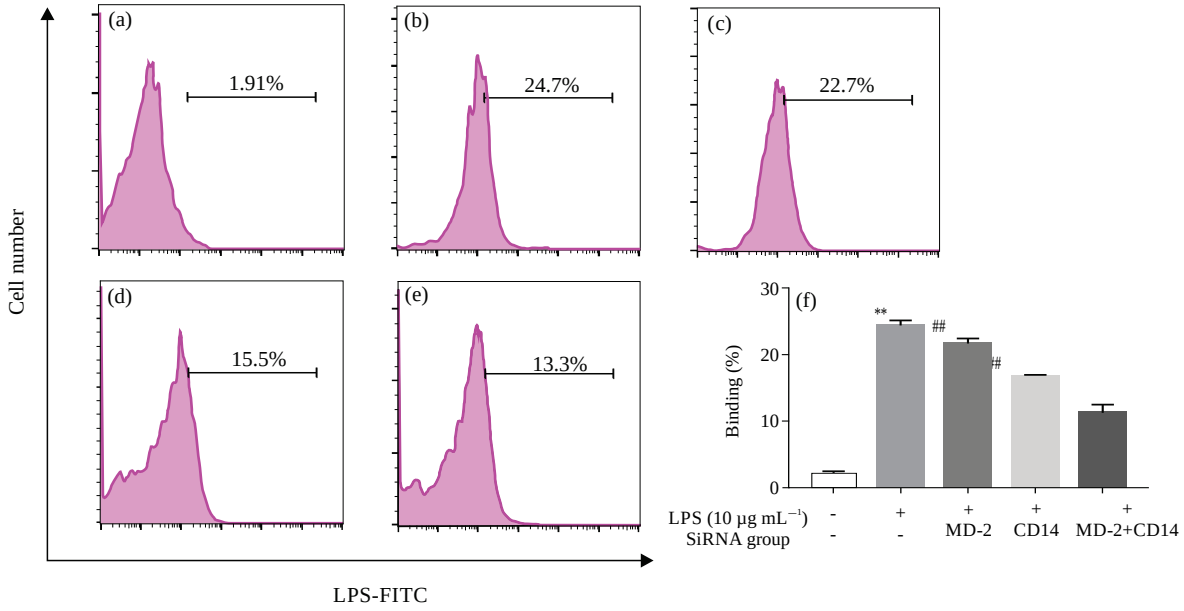

Fig. 2(a-f): Effect of CD14 and MD-2 on the binding activity of LPS to MECs receptor was detected by flow cytometry
A: Control group, B: LPS group, C: LPS+MD-2 siRNA group, D: LPS+CD14 siRNA group, E: LPS+CD14+MD-2 siRNA group. Data are expressed as the Mean±SD and were analyzed by one-way ANOVA with a post hoc test, **p<0.01, compared with the control group, ##p<0.01, compared with the LPS group

Study on molecular docking of CD14 and MD-2: For CD14 proteins, CGA is buried in the LPS binding region of the NH_2-terminal pocket of CD14 (Fig. 4a, b). There is a strong hydrogen bond between the phenolic hydroxyl group of CGA and the NH_2-terminal residue ALA A29 and there are π-sulphur and π-sigma between the benzene ring of CGA and the residues of CYS A32 and LEU A94 in the NH_2-terminal pocket and there are many van der Waals forces between CGA and CD14 hydrophobic pockets. For MD-2 proteins, CGA is inserted into the hydrophobic pocket of MD-2 by hydrogen bond (SER C47), (VAL C63) and sulfur (CYS C25, ILE C32) (Fig. 4c, d). This suggests an interaction between CGA and these two proteins, especially CD14.

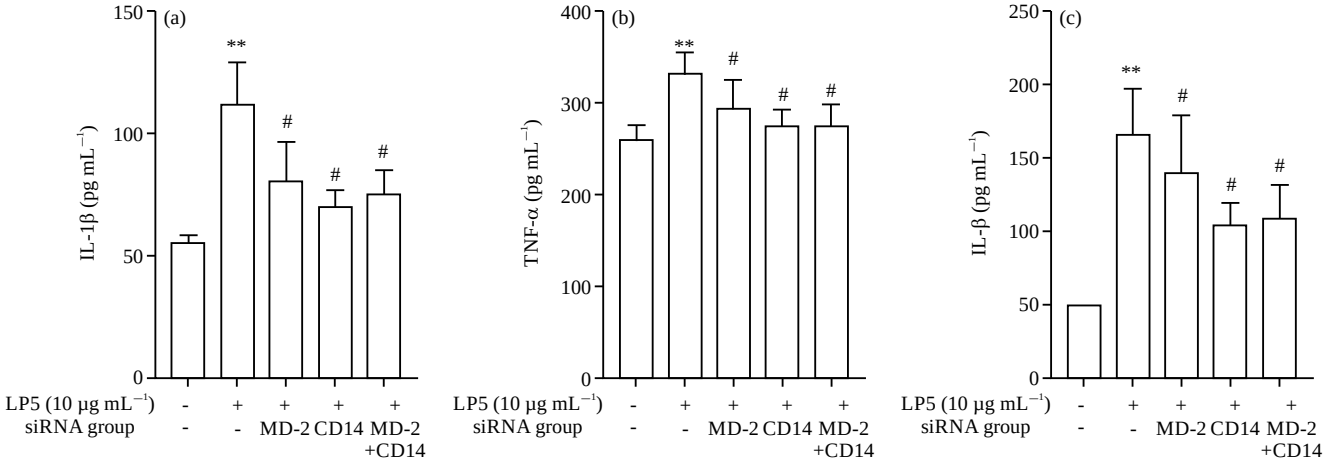

Fig. 3(a-c): Effect of CD14 and MD-2 on LPS-treated mouse MECs secretion of (a) IL-1β, (b) TNF-α and (c) and IL-6

Contents of IL-1β, TNF-α and IL-6 were measured (n = 4) in the culture supernatants by ELISA. Data are presented as the Mean ± SD of three independent experiments and were analyzed by one-way ANOVA with a post hoc test, **p<0.01, compared with the control group, #p<0.05, ##p<0.01, compared with the LPS group

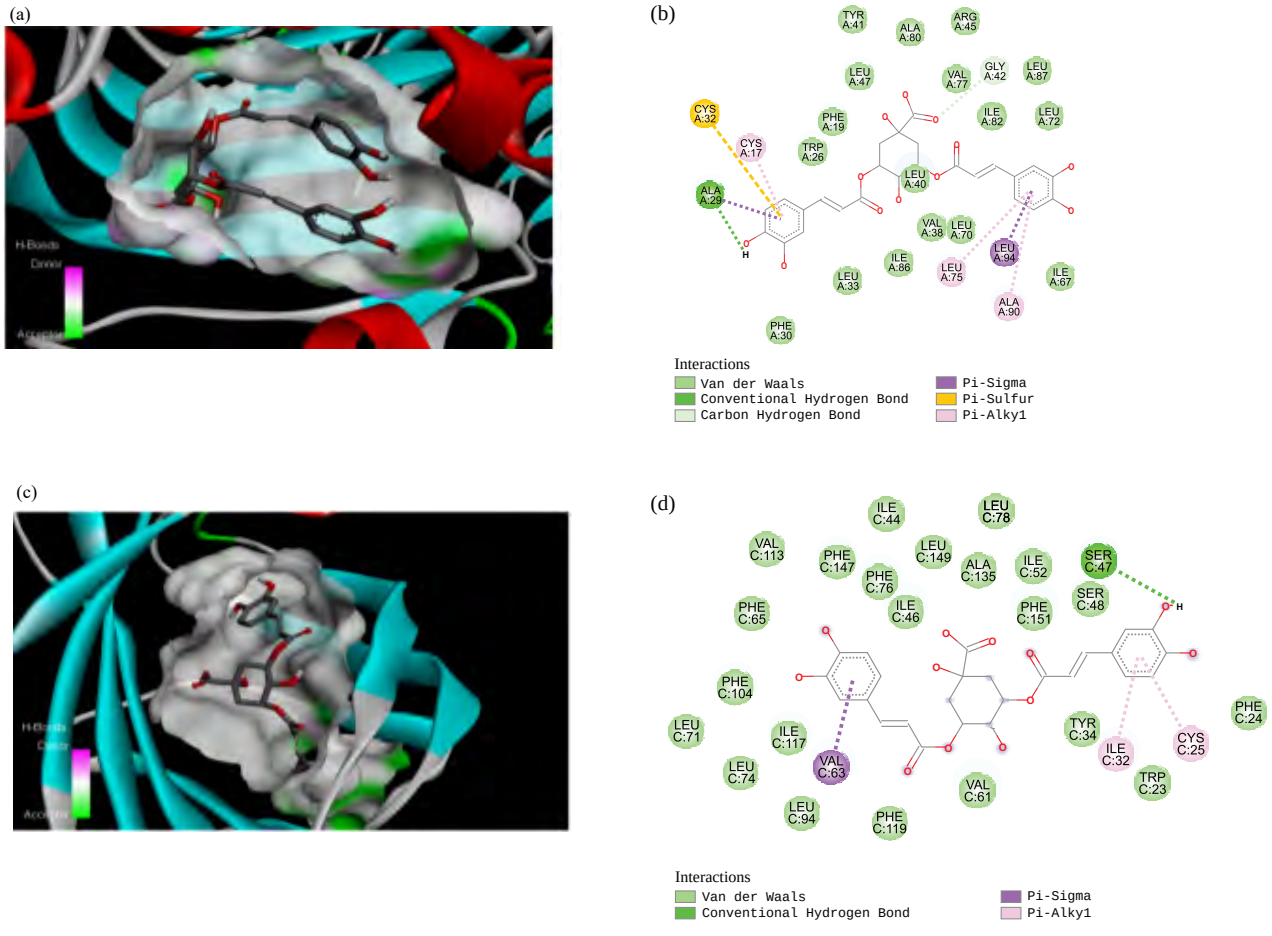

Fig. 4(a-d): 3D model and 2D model of the interaction between simulated CGA and the active site of CD14 protein (a-b), 3D model and 2D model of the interaction between simulated CGA with the active site of MD-2 (c-d)

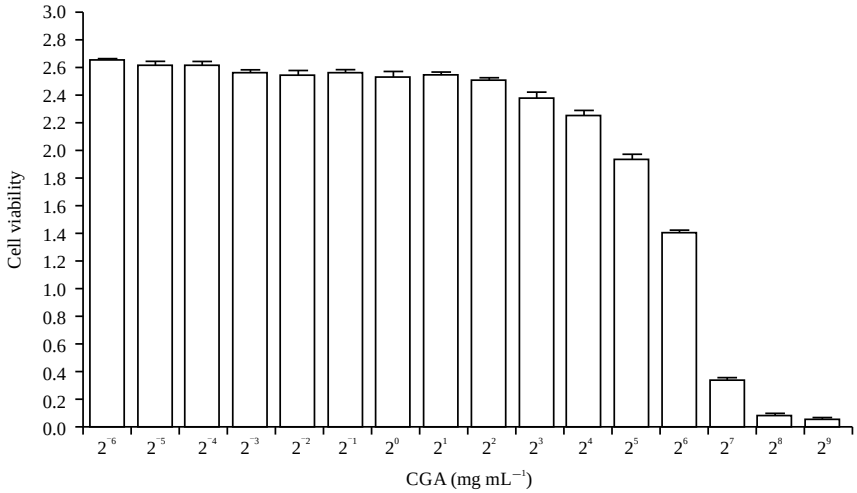

Fig. 5: Cell viability of CGA on MEC

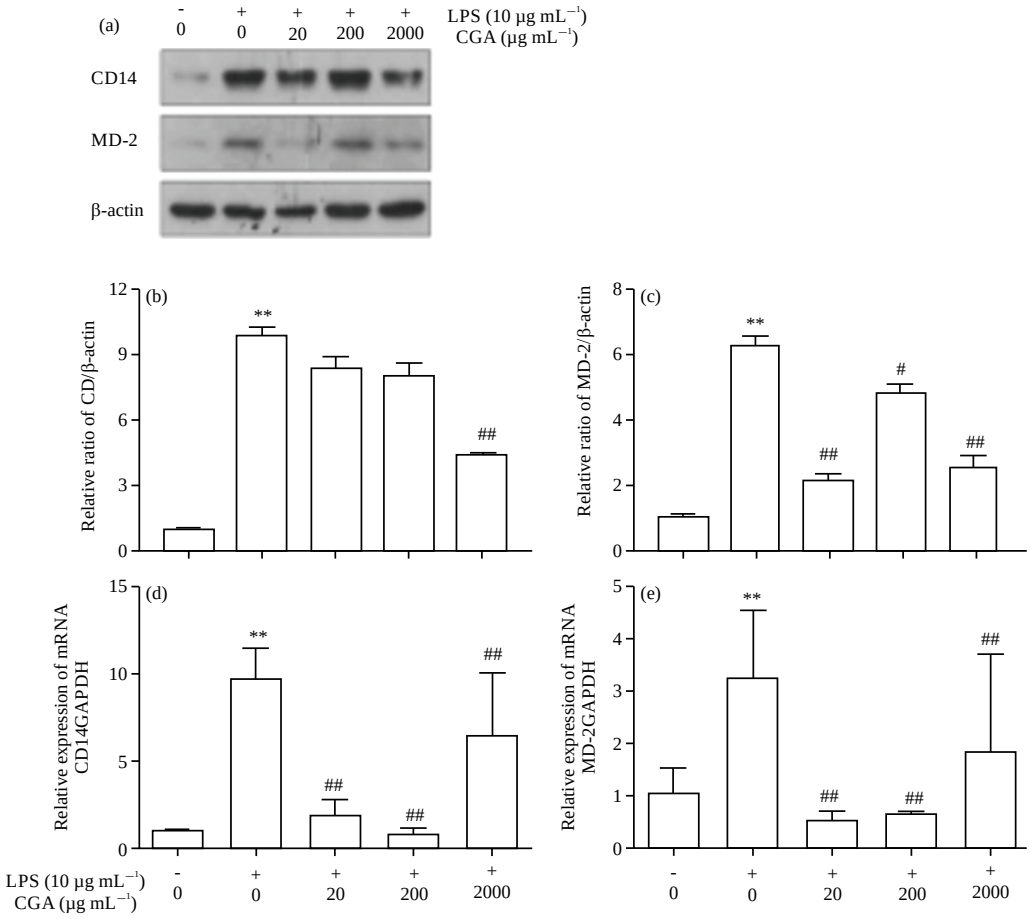

Fig. 6(a-e): RT-PCR and western blot expression of CD-14 and MD-2 (a) Effect of CGA on the mRNA expressions of CD-14 (b-d) and MD-2 (c-e) in each treatment group

Expression of CD-14 and MD-2 were measured (n = 3) by RT-PCR and western blot. Data are presented as the Mean±SD of three independent experiments and were analyzed by one-way ANOVA with a post hoc test, **p<0.01, compared with the control group, ##p<0.01, compared with the LPS group

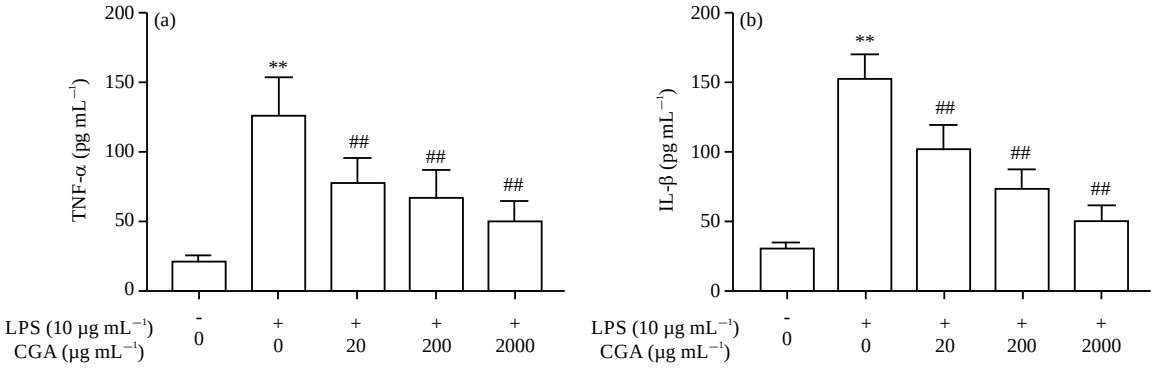

Fig. 7(a-b): Effect of CGA on TNF-α (a) and IL-6 (b) and secretion by mouse MECs treated with LPS

Contents of TNF-α and IL-6 were measured (n = 4) in the culture supernatants by ELISA. Data are presented as the Mean±SD of three independent experiments and were analyzed by one-way ANOVA with a post hoc test, **p<0.01, compared with the control group, ##p<0.01, compared with the LPS group

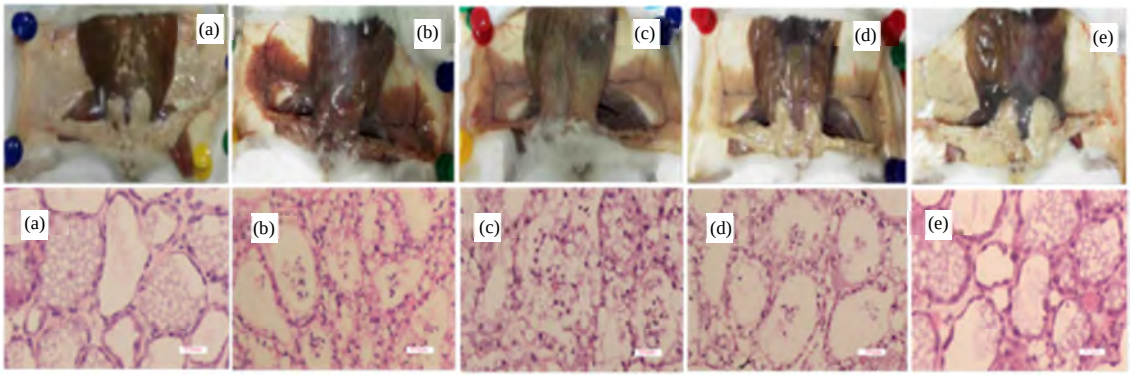

Fig. 8(a-d): Effect of CGA on LPS-induced mammary gland inflammation in mice.

The sections of the mammary gland collected from experimental mouse euthanized at the end of drug treatment were stained with hematoxylin and eosin and observed under light microscope. All pictures were taken from these sections, a: Normal mouse, b: Mouse treated with LPS alone, c: Mouse treated with LPS+20 mg mL^{-1} CGA, d: Mouse treated with LPS+40 mg mL^{-1} CGA, e: mouse treated with LPS+80 mg mL^{-1} CGA. Magnification on the Figure: (A–E) 400×

Effects of CGA on the cytotoxicity of mouse MECs: The cell activity of different concentrations of CGA was evaluated. The IC_{50} value of CGA in mouse MECs was 40.195 mg mL^{-1} and as the CGA concentration increased, the cell survival rate decreases, indicating a high inhibition of cell growth (Fig. 5). CGA high, medium and low concentration (2000, 200 and 20μg mL^{-1}) cell survival rate is higher.

Effects of CGA on LPS-induced CD-14 and MD-2 expression in MECs: Then we investigated the effect of CGA on LPS-induced CD14 and MD-2 expression in MECs. The expressions of CD14 and MD-2 in MECs were significantly increased upon LPS stimulation($p<0.01$) and CGA treatment significantly reduced the expression of CD14 and MD-2 ($p<0.01$) (Fig. 6).

Effects of CGA on LPS-induced secretion of TNF-α and IL-6 from MECs: Because the release of cytokines is considered to reflect inflammatory responses, the effect of CGA on LPS-induced inflammation in MECs was evaluated by measuring the secretion levels of proinflammatory cytokines. As shown in Fig. 7, LPS stimulation significantly induced the releases of TNF-α (Fig. 7a) and IL-6 (Fig. 7b) in MECs ($p<0.01$). However, CGA treatment significantly reduced the LPS-induced secretions of TNF-α and IL-6 ($p<0.01$).

Histopathologic changes of mammary gland tissue: Based on the macroscopic pathology and histological changes, hemorrhage and inflammatory infiltration were rare in the control mice, the mammary gland tissues were milky white and soft (Fig. 8a) and the mammary acinar had a unique shape and size (Fig. 8a). However, in the LPS group, mammary gland

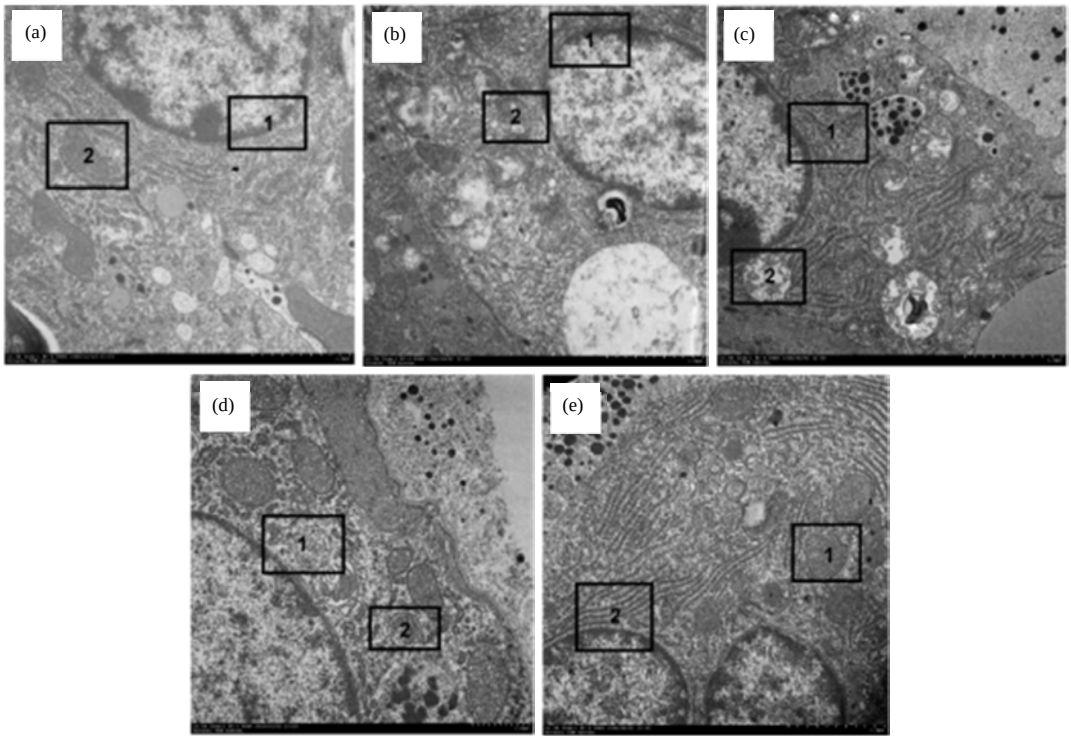

Fig. 9(a-e): Effect of CGA on LPS-induced mouse mammary gland cell structure

a: Normal mouse, b: Mouse treated with LPS alone, c: Mouse treated with LPS+20 mg mL^{-1} CGA, d: Mouse treated with LPS+40 mg mL^{-1} CGA, e: Mouse treated with LPS+80 mg mL^{-1} CGA

tissues presented evident edema, inflammatory hyperemia, milk stasis and local tissue necrosis (Fig. 8b). The structure of the mammary gland was significantly disrupted and contained cell debris, mucus, fibrin, exfoliated epithelial cells and large amounts of neutrophils in the acinar cavity. Besides, the acinar septum was thickened and the infiltration of inflammatory cells and hemorrhage were observed (Fig. 8b). CGA treatment significantly ameliorated the LPS-induced macroscopic changes in a dose-dependent manner (Fig. 8c, e). Fewer neutrophils were observed in the alveolar lumen, the mammary alveoli were thinner and mammary hyperemia and edema were dose-dependently attenuated (Fig. 8c, e).

TEM observations: There were no typical ultrastructural changes in the control group (Fig. 9a). For example, the cell wall was uniform, the cytoplasmic matrix was abundant and the organelle-rich cytoplasm included mitochondria, Golgi apparatus, vacuole, liposomes and the nucleus. In the presence of LPS (Fig. 9b), ultra structural changes were observed including unclear boundaries of the nucleus (Fig. 9b-1). The numbers of mitochondria were decreased significantly and gathered. Both the inner and outer membrane of mitochondria were dilated and mixed so it was difficult to distinguish the double structure. The cristae of the mitochondria had disappeared. Furthermore, the matrix was turbid and contained vacuoles, the rough endoplasmic reticulum was slightly dilated and cleaved into vesicles and parts of ribosomes were shed into the cytoplasm (Fig. 9b-2). Treatment with CGA significantly ameliorated the LPS-induced ultrastructural changes in a dose-dependent manner (Fig.9c-e). The damaged mitochondria and rough endoplasmic reticulum were attenuated as assessed by histology and fewer irregularly shaped vacuoles and holes were seen in the cytoplasm, which was also dose-dependent. For example, there are still a large number of unclear boundaries of the nucleus, the matrix was turbid and contained vacuoles, the rough endoplasmic reticulum was slightly dilated and cleaved into vesicles (Fig. 9c-1 and 2). With the dose of CGA is increased, the nuclear boundary became clear, the vacuoles in the cytoplasm were decreased, the cristae of the mitochondria were recovered and the number was increased (Fig. 9d-1 and 2). When treated with high doses of CGA, the damaged mitochondria and rough endoplasmic reticulum were attenuated and the nuclear membrane was clear (Fig.9e-1 and 2).

DISCUSSION

CD14 and MD-2 play an important role in the inflammatory signal transduction of extracellular LPS-TLR4. These two proteins can promote the transmission and recognition of LPS. It was reported that mice devoid of CD14 did not develop septic shock or accumulate pro-inflammatory cytokines in the blood following exposure to *E. coli* or intraperitoneal injection of LPS at a dose lethal to wild-type mice[28]. Similarly, knockout studies in mice have shown that MD-2 is an essential helper molecule in TLR4 signal transduction and mice lacking the MD-2 gene do not respond to LPS[11]. Our results showed that there was a certain amount of MD-2 protein expression on MECs, while the expression of CD14 protein was relatively low. After the expression of CD14 and MD-2 genes were inhibited alone or at the same time and then stimulated by fluorescent LPS, the binding rate of MECs to LPS and the release of cytokines in the transfection group were significantly lower than those in the control group, which indirectly proved that CD14 and MD-2 could promote the transmission of LPS on mouse MEC. Therefore, it is necessary to block the extracellular signal transduction of LPS by using CD14 and MD-2 as molecular targets of drugs.

The crystal structure shows that CD14 and MD-2 have almost the same size of the hydrophobic pocket for extraction and delivery of LPS. The NH_2-terminal hydrophobic pocket covering half of CD14 contains four separate regions (aa 26-32, 41-44, 56-64, 78-83), which are used to extract and transfer LPS[29,30]. Similarly, the hydrophobic residues at positions 82, 85 and 87 of MD-2 are essential both for the transfer of LPS from CD14 to monomeric MD-2 and for TLR4 activation[10]. Our molecular docking results show that there are multiple binding sites between CGA and CD14, such as A29, A32 and A94 etc., which almost cover four independent regions of LPS transmission. For MD-2, although the binding sites of CGA and MD-2 are different from those of LPS and MD-2, CGA has binding sites A25, A47, etc. in the MD-2 hydrophobic pocket. All in all, CGA may occupy the hydrophobic pockets of CD14 and MD-2 and hinder the extraction and transmission of LPS by CD14 and MD-2, thereby preventing LPS-TLR4 extracellular signal transmission and ultimately inhibiting the secretion of cytokines and the production of breast inflammation. Besides, CGA can significantly reduce LPS-induced increases in CD14 and MD-2 expression. However, the specific binding site of CGA to CD14 and MD-2 and the reason why CGA affects the expression of CD14 and MD-2 need to be further explored.

Recent evidence suggests that mitochondrial stress leads to inflammation and its dysfunction increases cytokine-induced chemotactic activity[31]. In this study, we found that LPS could cause the double membrane structure of MECs to be difficult to distinguish and the mitochondrial crest disappeared, while CGA could restore the damaged mitochondrial structure. Therefore, we speculated that the protective effect of CGA on MECs inflammation was related to the recovery of mitochondrial structure. Besides, our results show that CGA can reduce the increase of cytokines (IL-6, TNF-α) induced by LPS and then reduce the damage of cytokines to cells. The cytokine storm caused by novel coronavirus is fatal to the human body and it is of great significance to prevent the secretion of cytokines.

CONCLUSION

CGA may inhibit the production of inflammation in mouse mammary epithelial cells by targeting CD14 and MD-2, down-regulate the intracellular transduction of TLR4 signals, reduce the release of cytokines and reduce the excessive activation of mitochondria, thereby reducing the pathology of organelles.

SIGNIFICANCE STATEMENT

In this study, it was found that there are CD14 and MD-2 on mouse mammary epithelial cells and CD14 and MD-2 play an irreplaceable role in the extracellular signal transmission of LPS, while chlorogenic acid can target CD14 and MD-2. MD-2 inhibits inflammation in mouse mammary epithelial cells. Also, CGA can effectively inhibit the general changes in breast tissue caused by lipopolysaccharides, breast inflammatory cell infiltration, mitochondrial and rough endoplasmic reticulum damage, which will provide a certain reference for the development of natural anti-inflammatory drugs.

ACKNOWLEDGMENT

This study was supported by a grant from the National Natural Science Foundation of China (No. 31260618), (No. 31470128) and (No.31760747).

REFERENCES

1. Ulevitch, R.J. and P.S. Tobias, 1995. Receptor-dependent mechanisms of cell stimulation by bacterial endotoxin. J. Annu. Rev. Immunol., 13: 437-457.
2. Kelley, S.L., T. Lukk, S.K. Nair and R.I. Tapping, 2013. The crystal structure of human soluble CD14 reveals a bent solenoid with a hydrophobic amino-terminal pocket. J.I. 190: 1304-1311.

3. Kim, J.I., C.J. Lee, M.S. Jin, C.H. Lee, S.G. Paik, H. Lee and J.O. Lee, 2005. Crystal structure of CD14 and its implications for lipopolysaccharide signaling. J. Biol. Chem., 280: 11347-11351.
4. Viriyakosol, S., P.S. Tobias, R.L. Kitchens and T.N. Kirkland, 2001. MD-2 binds to bacterial lipopolysaccharide. J. Biol. Chem., 276: 38044-38051.
5. Schromm, A.B., E. Lien, P. Henneke, J.C. Chow and A. Yoshimura *et al*., 2001. Molecular genetic analysis of an endotoxin nonresponder mutant cell line: A point mutation in a conserved region of MD-2 abolishes endotoxin-induced signaling. J. Exp. Med., 194: 79-88.
6. Rallabhandi, P., J. Bell, M.S. Boukhvalova, A. Medvedev and E. Lorenz *et al*., 2006. Analysis of TLR4 polymorphic variants: New insights into TLR4/MD-2/CD14 stoichiometry, structure and signaling. J. Immunol., 177: 322-332.
7. Gay, N.J. and M. Gangloff, 2007. Structure and function of toll receptors and their Ligands. Ann. Rev. Biochem., 76: 141-165.
8. Medzhitov, R., P. Preston-Hurlburt and C.A. Janeway, 1997. A human homologue of the *Drosophila* toll protein signals activation of adaptive immunity. Nature, 388: 394-397.
9. Raetz, C.R. and C. Whitfield, 2002. Lipopolysaccharide endotoxins. Annu. Rev. Biochem., 71: 635-700.
10. Park, B.S., D.H. Song, H.M. Kim, B.S. Choi, H. Lee and J.O. Lee, 2009. The structural basis of lipopolysaccharide recognition by the TLR4–MD-2 complex. Nature, 458: 1191-1195.
11. Nagai, Y., S. Akashi, M. Nagafuku, M. Ogata and Y. Iwakura *et al*., 2002. Essential role of MD-2 in LPS responsiveness and TLR4 distribution. Nat. Immunol., 3: 667-672.
12. Ohto, U., K. Fukase, K. Miyake and Y. Satow, 2007. Crystal structures of human MD-2 and its complex with antiendotoxic lipid IVa. Science, 316: 1632-1634.
13. Resman, N., J. Vašl, A. Oblak, P. Pristovšek, T.L. Gioannini, J.P. Weiss and R. Jerala, 2009. Essential roles of hydrophobic residues in both MD-2 and toll-like receptor 4 in activation by endotoxin. J. Biol. Chem., 284: 15052-15060.
14. Hebeda, C.B., S.M. Bolonheis, A. Nakasato, K. Belinati and P.D.C. Souza *et al*., 2011. Effects of chlorogenic acid on neutrophil locomotion functions in response to inflammatory stimulus. J. Ethnopharmacol., 135: 261-269.
15. Stoclet, J.C., T. Chataigneau, M. Ndiaye, M.H. Oak, J. El Bedoui, M. Chataigneau and V.B. Schini-Kerth 2004. Vascular protection by dietary polyphenols. Eur. J. Pharmacol., 500: 299-313.
16. Olmos, A., R.M. Giner, M.C. Recio, J.L. Rios, J.M. Cerdá-Nicolás and S. Máñez, 2007. Effects of plant alkylphenols on cytokine production, tyrosine nitration and inflammatory damage in the efferent phase of contact hypersensitivity. Brit. J. Pharmacol., 152: 366-373.
17. Zhang, X., H. Huang, T. Yang, Y. Ye, J. Shan, Z. Yin and L. Luo, 2010. Chlorogenic acid protects mice against lipopolysaccharide-induced acute lung injury. Injury, 41: 746-752.
18. Xu, Y., J. Chen, X. Yu, W. Tao, F. Jiang, Z. Yin and C. Liu, 2010. Protective effects of chlorogenic acid on acute hepatotoxicity induced by lipopolysaccharide in mice. Inflamm. Res., 59: 871-877.
19. Feng, R., Y. Lu, L.L. Bowman, Y. Qian, V. Castranova and M. Ding, 2005. Inhibition of activator protein-1, NF-κB and MAPKs and induction of phase 2 detoxifying enzyme activity by chlorogenic acid. J. Biol. Chem., 280: 27888-27895.
20. Zheng, Z., L. Shi, Y. Sheng, J. Zhang, B. Lu and L. Ji, 2016. Chlorogenic acid suppresses monocrotaline-induced sinusoidal obstruction syndrome: The potential contribution of NFκB, Egr1, Nrf2, MAPKs and PI3K signals. Environ. Toxicol. Pharmacol., 46: 80-89.
21. He, C.L., Q. Yi, Y.F. Li, H. Yang and L. Wang, 2013. Toll-like receptor-4 but not toll-like receptor-2 mediates secretion of tumour necrosis factor α and interleukin-8 in lipopolysaccharide-stimulated mouse mammary epithelial cells. Bull. Vet. Inst. Pulawy, 57: 393-397.
22. Alper, S., R. Laws, B. Lackford, W.A. Boyd, P. Dunlap, J.H. Freedman and D.A. Schwartz, 2008. Identification of innate immunity genes and pathways using a comparative genomics approach. Proc. Nat. Acad. Sci., 105: 7016-7021.
23. Sathishkumar, N., S. Sathiyamoorthy, M. Ramya, D.U. Yang, H.N. Lee and D.C. Yang, 2012. Molecular docking studies of anti-apoptotic BCL-2, BCL-XL and MCL-1 proteins with ginsenosides from *Panax ginseng*. J.Enz. Inhib. Med. Chem., 27: 685-692.
24. Shishodia, S., S. Majumdar, S. Banerjee and B.B. Aggarwal, 2003. Ursolic acid inhibits nuclear factor-kappaB activation induced by carcinogenic agents through suppression of IkappaBalpha kinase and p65 phosphorylation: Correlation with down-regulation of cyclooxygenase 2, matrix metalloproteinase 9 and cyclin D1. Cancer Res., 63: 4375-4383.
25. Mosmann, T., 1983. Rapid colorimetric assay for cellular growth and survival: Application to proliferation and cytotoxicity assays. J. Immunol. Methods, 65: 55-63.
26. Pfaffl, M.W. and M. Hageleit, 2001. Validities of mRNA quantification using recombinant RNA and recombinant DNA external calibration curves in real-time RT-PCR. Biotech. Lett., 23: 275-282.
27. Zhang, X., Y. Wang, C. Xiao, Z. Wei, J. Wang, Z. Yang and Y. Fu, 2017. Resveratrol inhibits LPS-induced mice mastitis through attenuating the MAPK and NF-κB signaling pathway. Microb. Pathogen., 107: 462-467.

28. Haziot, A., E. Ferrero, F. Köntgen, N. Hijiya and S. Yamamoto *et al*., 1996. Resistance to endotoxin shock and reduced dissemination of gram-negative bacteria in CD14-deficient mice. Immunity, 4: 407-414.
29. Juan, T.S.C., E. Hailman, M.J. Kelley, L.A. Busse and E. Davy *et al*., 1995. Identification of a lipopolysaccharide binding domain in CD14 between amino acids 57 and 64. J. Biol. Chem., 270: 5219-5224.
30. Stelter, F., M. Bernheiden, R. Menzel, R.S. Jack, S. Witt, X. Fan, M. Pfister and C. Schutt, 1997. Mutation of amino acids 39-44 of human CD14 abrogates binding of lipopolysaccharide and *Escherichia coli*. Eur. J. Biochem., 243: 100-109.
31. Morizot, B., 2012. Chance: From metaphysical principle to explanatory concept. The idea of uncertainty in a natural history of knowledge. Prog. Biophys. Mol. Biol., 110: 54-60.